Dynamic Behavior of Freely Rising Buoyant Solid Spheres in Non-Newtonian Liquids

K. H. Dewsbury, D. G. Karamanev, and A. Margaritis
Dept. of Chemical and Biochemical Engineering, The University of Western Ontario, London, Ont., Canada, N6A 5B9

The results of the hydrodynamic study of rising solid spheres in non-Newtonian (pseudoplastic) fluids are reported. The hydrodynamic parameters including drag coefficient, trajectory of rise, and terminal velocity were determined. The behavior of free-rising spheres was compared to that of falling spheres in the same type of fluids to see if any differences exist. It was observed that rising solid spheres behave differently from falling solid spheres at higher Reynolds numbers in non-Newtonian (pseudoplastic) fluids. At high Reynolds numbers rising solid spheres display a spiraling motion, while falling spheres display a linear trajectory. The angle between the velocity vector and horizontal plane of the spiraling trajectory was 60°. The spiraling trajectory led to a drag coefficient that was more than two times higher for rising solid spheres than that established for falling spheres in the Newton's law range in a non-Newtonian (pseudoplastic) liquid. The first ever correlation is proposed to calculate the drag coefficient of freely rising light solid spheres in non-Newtonian (pseudoplastic) fluids.

Introduction

The first to systemically study particles falling in a fluid was Newton (1760), and in the last century the study of spherical particles falling in a liquid or air has been well documented (Khan and Richardson, 1987). However, until recently there have been almost no studies on buoyant spherical particles rising in a liquid. This was due to the inaccurate assumption that rising spherical particles would have the same drag curve as falling spherical particles for a wide range of Reynolds numbers (Shapiro, 1961).

For falling spheres at higher Reynolds numbers, the drag coefficient is nearly constant at 0.44 for Newtonian fluids (Clift et al., 1978), and approaches a value of 0.44 for non-Newtonian fluids (Chhabra, 1993). However, it was recently discovered that the drag coefficient for rising spheres at higher Reynolds numbers is equal to 0.95 in Newtonian liquids (Karamanev and Nikolov, 1992). The assumption that rising and falling spheres would have the same drag coefficient at higher Reynolds numbers is based on the premise that the same forces, but in opposite direction, are applied on both rising and falling spheres and that their drag coefficient is equal as well. This assumption has proven to be inaccurate for Newtonian fluids (Karamanev and Nikolov, 1992).

Correspondence concerning this article should be addressed to D. G. Karamanev.

It is well known that for spherical particles the drag coefficient, C_D, is a sole function of the Reynolds number, and this relationship is called a drag curve. Considering that the drag curve is used to predict the terminal velocity of spherical particles, which is important for many types of industrial and other processes, a large error in the drag coefficient will lead to very inaccurate terminal velocity estimations, as shown in Eq. 1:

$$U_t = \sqrt{\frac{4gd|\rho_p - \rho_l|}{3\rho_l C_D}} \quad . \tag{1}$$

The difference in the hydrodynamic behavior between falling and rising spheres at higher Reynolds numbers is the result of the effect of turbulence on particle motion. It is known that at Reynolds numbers above approximately 130 the phenomena of wake shedding and rotation is apparent (Torobin and Gauvin, 1959). Wake shedding leads to an imbalance of the nonvertical forces acting on a particle. Depending on the properties of the particle, such as volume and density, this force imbalance may lead to a horizontal component of velocity and a nonlinear trajectory. Since falling

spherical particles have a density greater than the surrounding fluid, they are able to resist this force imbalance due to their high mechanical inertia and usually display a linear trajectory. However, rising spherical particles that have densities much less than that of the surrounding fluid have a low mechanical inertia and the force imbalance caused by wake shedding results in a spiraling trajectory. This spiraling trajectory is the main reason rising spheres that have the same diameter and $\Delta\rho$ as a falling sphere have more than double the drag coefficient at higher Reynolds numbers in Newtonian fluids.

In reviewing all current and past literature in the field of particle motion in non-Newtonian fluids, no studies on the rise of light solid spheres in non-Newtonian liquids have been found. This lack of information and the fact that non-Newtonian fluids are becoming more important in the chemical and biochemical industry (Margaritis and Zajic, 1978; Margaritis and Pace, 1986) were the main reasons for undertaking this research. This work will be important for modeling processes that involve bubbles rising in non-Newtonian fluids (Margaritis et al., 1999) as well as inverse fluidization with non-Newtonian liquids.

The main aim of this work is to study the hydrodynamic characteristics, and in particular the drag coefficient, terminal velocity, and particle trajectory, of free rising solid buoyant spheres in non-Newtonian (pseudoplastic) liquids as a function of the particle properties (diameter and density) and the fluid rheology.

Mathematical Description

The forces acting on a rising or falling sphere are:

- Gravity force:

$$F_g = V\rho_p g. \tag{2}$$

- Buoyancy force:

$$F_B = V\rho_l g. \tag{3}$$

- Drag force:

$$F_D = C_D \rho_l S\left(U_t^2/2\right). \tag{4}$$

The balance of these forces for steady-state terminal velocity is shown in Eq. 5:

$$C_D \rho_l S \frac{U_t^2}{2} = V|\rho_p - \rho_l| g. \tag{5}$$

Using a spherical geometry, the drag coefficient is calculated by rearranging Eq. 5:

$$C_D = \frac{4gd\Delta\rho}{3\rho_l U_t^2}. \tag{6}$$

The Reynolds number for solid spheres in a Newtonian fluid is given by

$$Re_t = \frac{\rho_l d U_t}{\mu}. \tag{7}$$

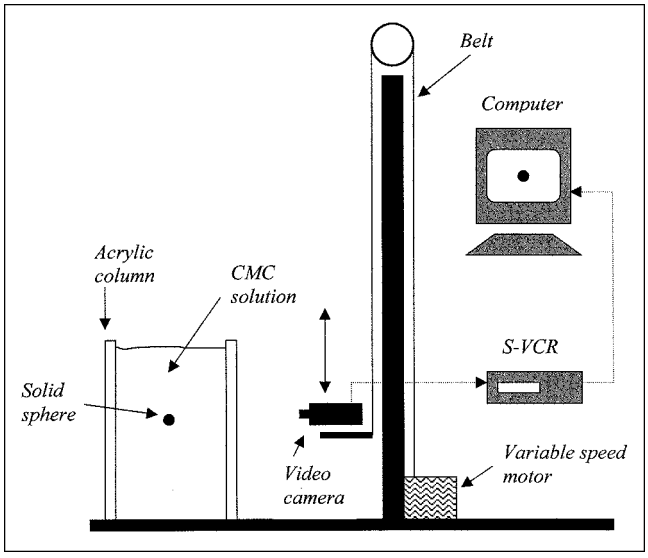

Figure 1. Experimental setup.

The apparent viscosity for a non-Newtonian power-law fluid is defined as:

$$\mu_a = m\gamma^{n-1}. \tag{8}$$

The shear rate of a rising solid sphere can be estimated by (Lali et al., 1989):

$$\gamma = \frac{U_t}{d}. \tag{9}$$

Combining Eqs. 7, 8 and 9, the Reynolds number for solid spheres in a non−Newtonian fluid is given by Eq. 10 (Lali et al., 1989):

$$Re_t = \frac{\rho_l d^n U_t^{2-n}}{m}. \tag{10}$$

Materials and Methods

Apparatus setup

Figure 1 shows the experimental setup used for this study. Two columns, one with a height of 130 cm and length and width of 80 cm, and another with a height of 240 cm and length and width of 30 cm were constructed using acrylic. The large width of the first column was required to eliminate wall effects that may hinder the velocity of larger spheres (Machac and Lecjaks, 1995). A special clamp allowed the solid spheres to be transported and released near the bottom of the column. The spheres were released 3 min after being brought down to the bottom of the column to ensure the liquid was quiescent.

To determine the terminal velocity and trajectory of the rising solid spheres, a high-resolution CCD video camera (Hitachi Ltd., Japan, model KP-M 1U) was used. The camera had the ability to be set at different heights along the column using a motorized pulley system. The video signal was recorded on a high-resolution Super-VHS video-recording

unit (Sanyo Canada Inc., model TLS-7000). To convert the analog video signal into a digital format, a frame grabber board (Miro Computer Products AG, Germany, model DC-30) was installed in a Pentium personal computer. This allowed the data that was stored on the S-VHS videotape to be sent to the computer and digitized for further processing. To perform a detailed analysis of the digital images, a software package (SigmaScan Pro 4.0, SPSS Inc., U.S.A.) was utilized. The geometry, trajectory, and velocity of particles with a vertical axis of symmetry are accurately determined using this software.

Terminal velocities of the rising spheres were determined by analyzing successive images from the S−VHS recording unit. A linear calibration was performed by taking a picture of a ruler located along the vertical axis of trajectory of the rising sphere. The imaging software was then used to calibrate the distance in the field of focus being used to obtain the pictures. Each frame the S-VHS records has a time interval of 0.01667 s. Therefore, knowing the distance the sphere traveled in a particular number of frames and the amount of time per frame allowed the determination of the terminal velocity. Using this procedure the terminal velocity of the sphere could be calculated with an error less than 1%. Once the velocity had been determined the drag coefficient and Reynolds number could be calculated.

Spheres trajectory images were created by using a stroboscope and a photographic camera with a manual shutter opening. The stroboscope allowed the sphere motion to be recorded at the desired time interval (0.045 s).

Materials

The solid-sphere material used in this work was mainly expanded polystyrene, but there were also spheres constructed with polyethylene, cork, and wood. Their diameters ranged from 3 mm to 60 mm and their densities ranged from 40 kg/m^3 to 900 kg/m^3. In this study, a solution of carboxymethylcellulose (CMC) with different concentrations was used as the non-Newtonian (pseudoplastic) liquid. The temperature of all CMC solutions was 22°C. For every CMC concentration, the density of the solution was very close to the density of water at 22°C. This shows that the concentration of CMC has little effect on the liquid density. A Bohlin rheometer (model VOR 200,000) was used to determine the rheological properties for the different concentrations of CMC. The usual range of shear rates used to determine the fluid rheology was 9−1,500 s^{-1}. The shear rates around the rising spheres in this research fell within this range. The only exception was the very small spheres in the highly concentrated 0.8% w/w CMC solution. This was the result of limitations of the rheometer used. The rheological parameters of liquids used in this work are given in Table 1. It was found that all CMC solutions exhibited a power-law behavior within the limits of the shear rates used in this study.

Table 1. Rheological Properties of Carboxymethylcellulose

CMC Conc. % w/w	Flow Index n	Consistency Index m (Ns^n/m^2)
0.05	0.92	0.0075
0.20	0.70	0.095
0.40	0.68	0.244
0.65	0.53	0.860
0.80	0.52	1.590

Results and Discussion

Drag curve of rising solid spheres in non-Newtonian (pseudoplastic) liquids

It has been shown that the drag curve for falling spheres in non-Newtonian (pseudoplastic) liquids follows the standard drag curve, that is, it is similar to Stokes' law at low Reynolds numbers, $0.1 < Re_t < 1$, and at high Reynolds numbers the drag coefficient approaches a value of 0.44 (Chhabra, 1993). As shown in Figure 2 the drag curve for rising solid spheres in non-Newtonian (pseudoplastic) liquids is very similar to the drag curve for falling solid spheres in the same non-Newtonian (pseudoplastic) liquids at Reynolds numbers below 135. The rising spheres displayed a linear trajectory in this region. However, at higher Reynolds numbers there are differences between rising and falling spheres that become apparent. When Re_t is greater than 135 the drag coefficient of rising spheres stabilizes at 0.95. The constant drag coefficient coincided with a spiraling trajectory. However, for the 0.05% w/w CMC concentration, the constant drag coefficient for the rising spherical solids when Re_t is greater than 135 was only apparent for a solid-sphere density less than 800 kg/m^3. At densities greater than 800 kg/m^3, the rising spherical solids continued to follow the standard drag curve (Eq. 11) as the Reynolds number increased until a critical Reynolds number where the drag coefficient begins to ''jump'' to the constant value of 0.95, as shown in Figure 2.

Since the correlation of Turton and Levenspiel (1986) best describes the standard drag curve (Karamanev, 1996), it can be used to calculate the drag curve of rising spheres when Re_t is less than 135:

$$C_D = \frac{24}{Re_t}\left(1 + 0.173\,Re_t^{0.657}\right) + \frac{0.413}{1 + 16{,}300\,Re_t^{-1.09}} \quad \text{for} \quad Re_t < 135. \quad (11)$$

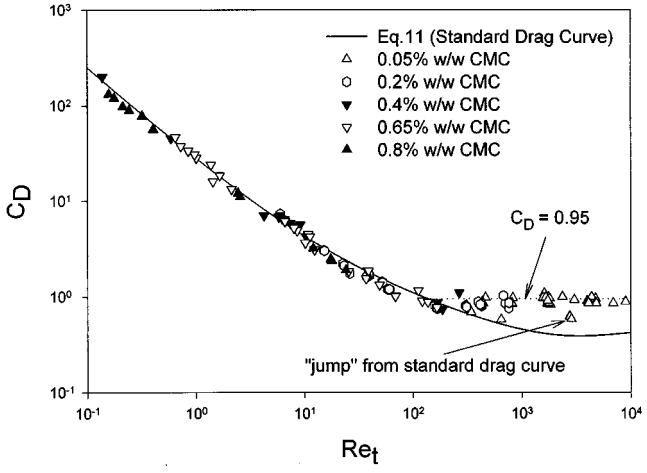

Figure 2. Drag coefficient vs. Reynolds number for rising solid spheres in aqueous carboxymethylcellulose.

When Re_t is greater than 135 and sphere density is low, the drag coefficient for rising solid spheres is given by

$$C_D = 0.95 \qquad \text{for} \quad Re_t > 135. \tag{12}$$

Trajectory of rising solid spheres

It was observed that when the drag coefficient for rising solid spheres in non-Newtonian (pseudoplastic) fluids was equal to a constant value of 0.95, the spheres displayed a spiraling trajectory. The spiraling trajectories had varying periods and amplitudes depending on the sphere diameter and density. It was calculated, however, that the angle between the velocity vector and horizontal plane was the same for each spiral and equal to $60° \pm 5\%$. The constant angle of 60° between the velocity vector and horizontal plane is very close to the value of 61° observed in Newtonian fluids (Karamanev and Nikolov, 1992). The 60° angle of rotation possibly results from the fact that the angle between the separating wake and the sphere is approximately 60°–70° (Torobin and Gauvin, 1959). This spiraling trajectory for different sphere diameters is shown in Figure 3. When Re_t is less than 135, all spheres exhibited a linear trajectory with a velocity vector angle of 90°. It was also observed that there were situations where the trajectory was neither linear nor spiraling. As shown in Figure 2, this occurred in the transition region where spheres with higher densities would "jump" from the standard drag curve when Re_t is greater than 135. In this transition regime there was unstable spiraling and sometimes a rectilinear trajectory observed. This leads to the possible conclusion that for different CMC concentrations and higher sphere densities, when Re_t is greater than 135 there is a critical Reynolds number where the effect of wake shedding becomes large enough to induce a spiraling ascending motion.

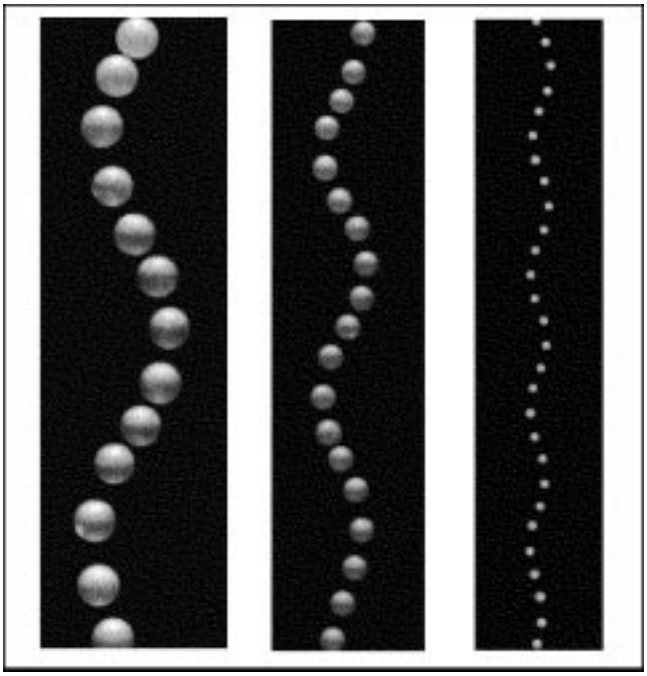

Figure 3. Trajectory of rising solid spheres in aqueous carboxymethylcellulose.

(a) Sphere diameter = 1.9 cm; sphere density = 40 kg/m^3; (b) sphere diameter = 1.1 cm; sphere density = 40 kg/m^3; (c) sphere diameter = 0.44 cm; sphere density = 40 kg/m^3.

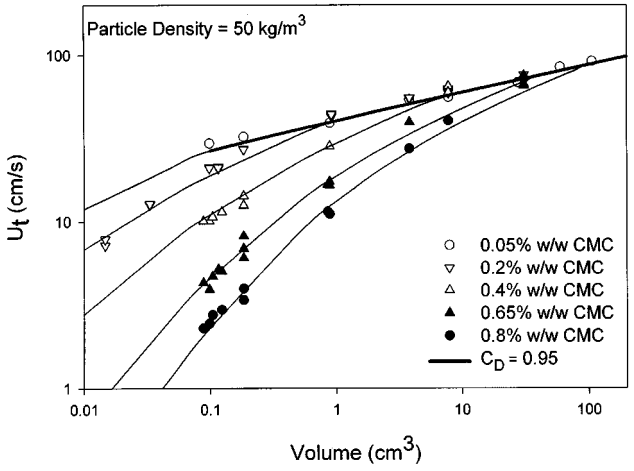

Figure 4. Terminal velocity vs. volume for rising solid spheres in aqueous carboxymethylcellulose.

Terminal velocity of rising solid spheres

Figure 4 displays the terminal velocity of the rising spheres as a function of their volume. A constant density of 50 kg/m^3 was used while varying the sphere diameter and the fluid rheology. The experimental data are plotted against the predicted theoretical data, which were calculated using Eqs. 6, 10, 11, and 12. Since this set of equations cannot be solved analytically, an iterative numerical procedure was applied using MS Excel software. A good fit between the experimental data and theoretical curves can be observed in Figure 4.

The terminal velocity-vs-volume results for the low concentration of CMC (0.05% w/w) is a linear relationship in logarithmic scale and independent of the fluid rheology even at very small volumes (0.1 cm^3). This is related to the fact that at this CMC concentration the drag coefficient for the volume of spheres studied (0.1 cm^3 to 100 cm^3) is constant at a value of 0.95. This was also associated with Reynolds numbers greater than 135.

When the drag coefficient is not constant, and the Reynolds number is less than 135, the volume-vs.-velocity relationship for all CMC concentration is nonlinear on a logarithmic scale. However, the curves become linear again at very low Reynolds numbers, when Stokes' law applies. For CMC concentrations greater than 0.05%, the nonlinear relationship was apparent as the sphere volume increased until the drag coefficient became constant at 0.95, as shown in Figure 4. At this point, the terminal velocity-vs.-volume curves became linear and deviated to the curve for the 0.05% w/w CMC solution. These results indicate that on a logarithmic scale, the nonlinear standard drag curve when Re_t is less than 135 corresponds to a nonlinear velocity–volume relationship.

It was also observed that as the CMC concentration was increased, the terminal velocity of a sphere at a constant volume and density would decrease significantly. This is indicative of the viscous effects of the concentrated CMC solutions when Re_t is less than 135.

Drag coefficient of rising solid spheres

The relationship between the diameter of a sphere and its drag coefficient at a constant density of 50 kg/m^3 and at varying CMC concentrations is shown in Figure 5. It is apparent that when the Reynolds number is less than 135, where the drag coefficient is greater than 0.95, there is a nonlinear relationship in logarithmic scale between the drag coefficient and sphere diameter. However, the relationship is linear at very low Reynolds numbers, in the Stokes regime. For the low CMC concentration of 0.05% w/w, the drag coefficient was constant at 0.95 or all diameters studied (0.4 cm to 6 cm). For all CMC concentrations above 0.05% w/w and sphere density of 50 kg/m^3, the drag coefficient vs. diameter curve became linear when Re_t is greater than 135. The experimental data points were very close to the theoretically predicted data as well.

The relationship between the diameter of a sphere and its drag coefficient at a constant CMC concentration of 0.05% w/w and varying particle densities is shown in Figure 6. For sphere diameters greater than 0.4 cm and a sphere density less than 800 kg/m^3, the drag coefficient was constant at 0.95 with a scatter of $\pm 15\%$ when Re_t is greater than 135. However, for sphere densities greater than 800 kg/m^3, the spheres followed the standard drag curve when Re_t is greater than 135 and the drag coefficient is below 0.95 until a critical Reynolds number where the drag coefficient began to approach the constant value of 0.95, as shown in Figure 6. Similar results have also been observed in Newtonian fluids (Karamanev et al., 1996). These results show that in a non-Newtonian (pseudoplastic) fluid, as the density of a rising sphere becomes close to that of the surrounding liquid, it becomes less influenced by wake shedding and the trajectory remains linear even when Re_t exceeds 135.

Conclusions

The main conclusions obtained from this study are:

1. The drag curve for rising solid spheres in non-Newtonian (pseudoplastic) liquids can be represented by the standard drag curve given by Turton and Levenspiel (1986) when Re_t is less than 135. When Re_t is greater than 135 and the particle density is low, the drag coefficient is constant at a value of 0.95.

2. The drag coefficient for a rising solid sphere in a non-Newtonian (pseudoplastic) liquid is significantly affected by its trajectory. At Reynolds numbers above 135 when the motion of a rising sphere was spiraling, the drag coefficient was more than two times greater than what is established for falling spheres that display a linear trajectory. This can be explained by the fact that spheres with a density greater than that of the surrounding fluid have a high degree of mechanical inertia that can resist the effects of wake shedding on its motion even at high Reynolds numbers. Rising spheres with lower densities do not have enough mechanical inertia to avoid the effects of wake shedding at higher Reynolds numbers and display a spiraling trajectory.

3. For spheres with a spiraling trajectory, the angle between the velocity vector and horizontal plane was always equal to $60° \pm 5\%$. When the sphere trajectory was linear, the angle between the velocity vector and horizontal plane was equal to 90°.

4. The logarithmic relationship between the terminal velocity of a rising sphere and its volume is nonlinear when Re_t is less than 135. However, the relationship is linear at very low Reynolds numbers, when Stokes' law applies, and when Re_t is greater than 135 and $C_D = 0.95$.

5. The logarithmic relationship between the drag coefficient and sphere diameter is nonlinear when Re_t is less than 135. However, the relationship is linear at very low Reynolds numbers, in the Stokes regime, and when Re_t is greater than 135 and $C_D = 0.95$.

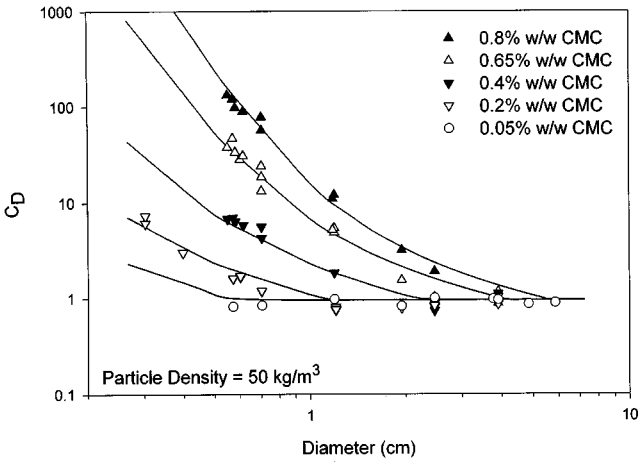

Figure 5. Drag coefficient vs. diameter at constant density for rising solid spheres in aqueous carboxymethylcellulose.

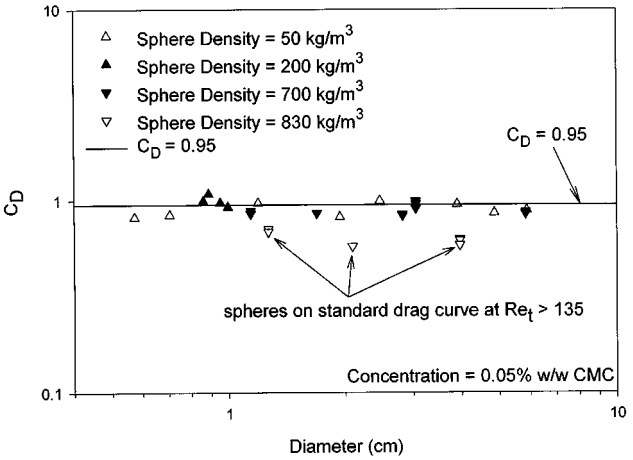

Figure 6. Drag coefficient vs. diameter at constant carboxymethylcellulose concentration for rising solid spheres.

Acknowledgments

This work was supported by the Academic Development Fund (ADF) of the University of Western Ontario and also by individual research grants awarded to two of the authors (D. K. and A. M.) by the Natural Sciences and Engineering Research Council of Canada (NSERC). The assistance of Greg Snell at 3M Canada Inc. in the measurement of the rheological properties of our solutions is greatly appreciated.

Notation

d = diameter, m
g = acceleration due to gravity, m/s^2
S = surface area projected onto a horizontal plane, m^2
V = particle volume, m^3

Greek letter

ρ_l = liquid density, kg/m^3
ρ_p = solid-sphere density, kg/m^3
$\Delta\rho$ = density difference between solid sphere and the surrounding liquid, kg/m^3
μ = viscosity of Newtonian liquid, Pa·s

Literature Cited

Chhabra, R. P., *Bubbles, Drops, and Particles in Non-Newtonian Fluids*, CRC Press, Boca Raton, FL (1993).

Clift, R., J. R. Grace, and M. E. Weber, *Bubbles, Drops, and Particles*, Academic Press, New York (1978).

Karamanev, D. G., and L. N. Nikolov, ''Free Rising Spheres Do Not Obey Newton's Law for Free Settling,'' *AIChE J.*, **38**, 1843 (1992).

Karamanev, D. G., C. Chavarie, and R. C. Mayer, ''Dynamics of the Free Rise of a Light Solid Sphere in Liquid,'' *AIChE J.*, **42**, 1789 (1996).

Karamanev, D. G., ''Equations For Calculation of the Terminal Velocity and Drag Coefficient of Solid Spheres and Gas Bubbles,'' *Chem. Eng. Commun.*, **147**, 75 (1996).

Khan, A. R., and J. F. Richardson, ''The Resistance to Motion of a Solid Sphere in a Fluid,'' *Chem. Eng. Commun.*, **62**, 135 (1987).

Lali, A. M., A. S. Khare, and J. B. Joshi, ''Behaviour of Solid Particles in Viscous Non-Newtonian Solution: Settling Velocity, Wall Effects and Bed Expansion in Solid-Liquid Fluidized Beds,'' *Powder Technol.*, **57**, 39 (1989).

Machac, I., and Z. Lecjaks, ''Wall Effect for a Sphere Falling Through a Non-Newtonian Fluid in a Rectangular Duct,'' *Chem. Eng. Sci.*, **50**, 143 (1995).

Margaritis, A., and G. W. Pace, ''Microbial Polysaccharides,'' *Comprehensive Biotechnology: The Practice of Biotechnology*, Vol. 3, H. W. Blanch, S. Drew, and D. I. C. Wang, eds., Pergamon Press, Oxford, p. 1005 (1986).

Margaritis, A., and J. E. Zajic, ''Mixing, Mass Transfer and Scale-Up of Polysaccharide Fermentations,'' *Biotechnol. Bioeng.*, **20**, 939 (1978).

Margaritis, A., D. W. Te Bokkel, and D. G. Karamanev, ''Bubble Rise Velocities and Drag Coefficients in Non-Newtonian Polysaccharide Solutions,'' *Biotechnol. Bioeng.*, **64**, 3, 257 (1999).

Newton, I., *Philosophiae Naturalis: Principia Mathematica*, Coloniae Allobrokum, Roma (1760).

Shapiro, A. H., *Shape and Flow: The Fluid Dynamics of Drag*, Doubleday, New York (1961).

Torobin, C. B., and W. H. Gauvin, ''Fundamental Aspects of Solids-Gas Flow,'' *Can. J. Chem. Eng.*, **37**, 167 (1959).

Turton, R., and O. Levenspiel, ''A Short Note on the Drag Correlation for Spheres,'' *Powder Technol.*, **47**, 83 (1986).

Manuscript received June 18, 1999, and revision received Sept. 23, 1999.